Evaluation of state-of-the-art geodetic GPS receivers for frequency comparisons

U. Weinbach, S. Schön
Institut für Erdmessung (IfE)
Leibniz Universität Hannover
Hannover, Germany
weinbach@ife.uni-hannover.de

T. Feldmann
Time and frequency division
Physikalisch-Technische-Bundesanstalt (PTB)
Braunschweig, Germany

***Abstract*—In this paper we show results of a test campaign, designed to investigate the stability of GPS receiver clocks locked to an external frequency source. Two types of geodetic receivers and one timing receiver have been compared. The receivers were operated in pairs in zero and short baseline setups with common reference frequency. Care was taken to minimize environmental effects. The observation data were processed using both a simple carrier phase single difference algorithm and the Bernese GPS Software 5.0 in Precise Point Positioning (PPP) mode. Some shortcomings of previous studies in terms of receiver equipment and the experimental setup of the short baseline could be avoided. It is shown that using geodetic receivers and the ionosphere-free linear combination of the carrier phase observations, frequency comparisons at a level of $\sigma_y(\tau)=2\cdot10^{-16}$ for averaging times of one day are feasible on a zero baseline, i.e. if all environmental effects are eliminated.**

I. INTRODUCTION

Apart from accurate positioning, geodetic GNSS receivers that are prepared to accept an external frequency input can be used for remote frequency comparisons of precision oscillators (e.g. H-Maser, Rb and Cs frequency standards) [1]. Furthermore, the ability to recover the stable signal of an external frequency standard in the GPS processing can be used to form an ensemble timescale, as it is done for example by the International GNSS Service (IGS) or the Bureau International des Poids et Mesures (BIPM) to derive the IGS timescales [2] and the Temps Atomique International (TAI) [3], respectively. For both applications it is essential that the receivers process the external frequency faithfully and do not degrade the stability of the external oscillator. Using GPS carrier phase observations and geodetic analysis techniques frequency comparisons at a level of $\sigma_y(\tau)=2\cdot10^{-15}$ for averaging times of one day are now regularly reported [4], [5]. In this study we aim to assess the lower limit for frequency comparisons set by the stability of the receiver hardware. There have been previous studies in this area, e.g. [6], [7], but these either focused on calibration issues or lacked a rigorous experimental setup.

We thank the Deutsche Forschungsgemeinschaft (DFG) and the centre for QUantum Engineering and Space Time research (QUEST), Hannover for funding this work

Currently most of the IGS stations equipped with hydrogen masers or other high-precision frequency standards are using rather old Ashtech ZXII receivers. This receiver type has been proven to be well suited for time and frequency transfer in various studies [8], [9]. However, in a few years time these receivers are likely to be replaced because they are not able to track new satellite signals (L2C, L5, Galileo) and support has ended some years ago. In order to assess the capability of alternative GPS receivers for high precision frequency comparisons, we performed test measurements with two pairs of geodetic GNSS receivers (JPS Legacy and Leica GRX1200GG Pro). These receivers can be prepared to accept an external frequency input. In the global IGS network there are currently three stations operating the JPS and the Leica receiver in combination with an active hydrogen maser (Tab.1). In addition, a pair of DICOM GTR50 GPS receivers was tested. The latter receiver type is specially designed for time transfer. Therefore it is prepared to accept an external 1 PPS input signal instead of a frequency signal. All three receivers are not calibrated, i.e. they can only be used for frequency comparisons but not yet for time transfer.

TABLE I. RECEIVERS USED IN THIS STUDY

Receiver	Input signal	No. of receivers at IGS stations with H-Maser
JPS Legacy	Ext. frequency	3
Leica GRX1200GG Pro	Ext. frequency	3
DICOM GTR50	External 1 PPS	Only time labs

Since we were interested in the stability of the receiver clocks at the pico-second level, this paper focuses on the carrier phase measurements. The stability of the code derived receiver clock must be dealt with separately. Furthermore, we restrict our analysis to GPS.

The primary objectives of our investigation can be summarized by the following key questions:

- Are there significant differences with respect to the handling of the external clock signal among the test receivers?
- What is the ultimate stability of the receiver hardware in a temperature stabilized environment?
- What is the influence of multipath?

II. EXPERIMENTAL SETUPS

In order to be able to control the environmental effects on the GPS observations, the receivers have been operated in zero and short baseline configurations (Fig. 1). This way we were able to effectively separate distance dependent errors (e.g. atmospheric propagation delays) and site specific errors (e.g. multipath) from the pure receiver measurement performance. In addition, an operation with common clock has the unique advantage that the differential receiver clock offset is known (in theory) to be constant as long as the receivers are locked to the signal of the external oscillator. The 10 MHz reference frequency and the 1 PPS signal were derived from the active Hydrogen Maser PTB H6 (VCH-1003A). The internal clock steering of the receivers has been disabled. The maser frequency was distributed using an HPDA-15RM-E amplifier by Spectra Dynamics. In the zero baseline setup, the receivers were connected to the same antenna via one signal splitter (Mod. ALDCBS, GPS Networking Inc.), in case of the short baseline two identical signal splitters were used to connect the receivers to two antennas approximately 4.3 metres apart on the roof of the Kopfermann Bau at PTB (Fig. 2). The receivers were operated in a laboratory, which is supposed to be temperature-stabilized to 0.5 K. In order to minimize temperature influences on the short baseline HELIAX^{TM}-type antenna cables (FSJ2-50, Andrew Corp.) have been employed. In both experimental setups we used Leica AX1202 antennas and the GPS observation data was recorded at a sampling interval of 1 Hz.

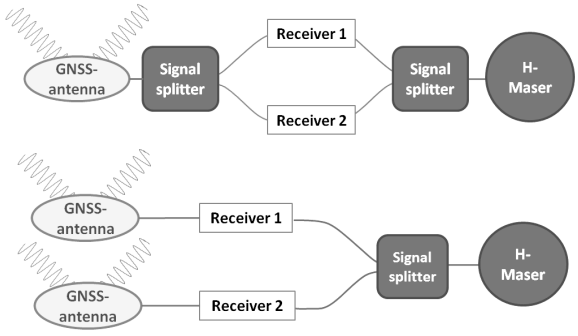

Figure 1. Zero (top) and short (bottom) baseline setups with common clock

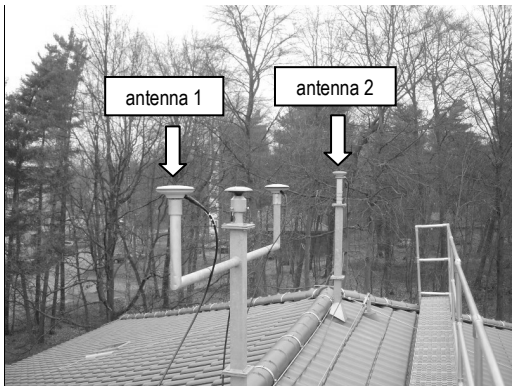

Figure 2. Antenna installation on the roof at PTB

III. PROCESSING SCHEMES

In order to extract the differential clock error of the two receivers, the data were processed using two different strategies, a simple differential approach based on carrier phase single differences and a Precise Point Positioning solution, computed with the Bernese GPS Software 5.0.

A. The single difference approach

Forming single differences between the observations of one satellite observed by two receivers allows a direct comparison of the clock offset of the two receivers without any parameter estimation. This approach is commonly referred to as Common–View method. In order to understand the elimination of the different error sources in the GPS measurements by the experimental setups we will briefly review the GPS observation equation. Both, L1 and L2 carrier phase observations (in metres) of a satellite j observed by a receiver A can be written as

$$\Phi_A^j = \rho_A^j + c\left(\delta t_A - \delta t^j\right) + T_A^j - I_A^j + \lambda N_A^j + \delta_{\varphi,A} + \delta_\varphi^j + MP_A^j + PCV_A^j + \varepsilon_A^j \quad , \quad (1)$$

where Φ_A^j is the phase observation multiplied by the wavelength of the respective carrier frequency, ρ_A^j is the geometric distance containing satellite and receiver position, δt_A and δt^j are the receiver and satellite clock offsets, respectively. The term T_A^j designates the delay of the signal in the neutral part of the atmosphere (mainly the troposphere) and I_A^j the frequency dependent delay caused by the ionosphere. The wavelength of the carrier signal is represented by λ and the unknown integer ambiguity by N_A^j. The delays in the receiver and satellite hardware are $\delta_{\varphi,A}$ and δ_φ^i. Finally, MP_A^j, PCV_A^j and ε_A^j are multipath influences, receiver antenna phase center variations and measurement noise, respectively.

Forming differences between the observations of one satellite observed simultaneously by two receivers A and B leads to the following expression:

$$\Delta\Phi_{AB}^j = \Delta\rho_{AB}^j + c\Delta\delta t_{AB} + \Delta T_{AB}^j - \Delta I_{AB}^j + \lambda\Delta N_{AB}^j + \Delta\delta_{\varphi,AB} + \Delta MP_{AB}^j + \Delta PCV_{AB}^j + \Delta\varepsilon_{AB}^j \quad (2)$$

Note that the satellite clock offset and the satellite hardware delay are eliminated. In the special case of a very short baseline (SBL) all atmospheric propagation delays and orbit errors also cancel, because they can be considered identical for both receivers. The geometric term $\Delta\rho_{AB}^{j}$ can be computed from accurately known satellite and receiver coordinates and removed from the single differences. The phase centre variations ΔPCV_{AB}^{j} can either be eliminated using identical antennas, properly oriented, or by applying calibration values. That means, in addition to the differential receiver clock error, the differential hardware delays and the constant ambiguity term only site dependent errors (mainly multipath effects) and measurement noise remain

$$\text{SBL:}\quad \Delta\Phi_{AB}^{j} = c\Delta\delta t_{AB} + \Delta\delta_{\varphi,AB} + \lambda\Delta N_{AB}^{j} + \Delta MP_{AB}^{j} + \Delta\varepsilon_{AB}^{j}. \quad (3)$$

It is important to note, that temperature induced variations of the differential hardware delay $\Delta\delta_{\varphi,AB}$ in the antennas and cables can have a large impact on the single differences. We observed differential effects of more than 100 ps during a few hours. Obviously, this is an undesirable effect, if we want to assess the stability of the differential receiver clock offset $\Delta\delta t_{AB}$. By choosing identical antennas and antenna cables with low temperature sensitivity we could successfully eliminate the differential effect of temperature variations in our short baseline experiment.

On the zero baseline (ZBL) even the site dependent errors are eliminated and the differential hardware delays are reduced to the difference of the delays in the short cables driving the signal from the antenna splitter to the receiver. Because the cables connecting the antenna splitter with the receivers are located in the temperature stabilized laboratory the differential delay should stay constant, regardless of the antenna and antenna cable. Consequently, the expression for the single differences on a zero baseline reduces to

$$\text{ZBL:}\qquad \Delta\Phi_{AB}^{j} = c\Delta\delta t_{AB} + \Delta\delta_{\varphi,AB} + \lambda\Delta N_{AB}^{j} + \Delta\varepsilon_{AB}^{j}\ . \quad (4)$$

Inspecting (4), we can see that every variation of the single differences exceeding the measurement noise must be attributed to the handling of the external frequency inside the receiver. At this point, we assume constant receiver hardware delays and the absence of cycle slips.

In summary, by forming single differences we obtain for every satellite in view an estimate of the differential receiver clock error biased by the differential hardware delay (identical for all satellites) and a satellite specific integer number of carrier phase cycles. In a straightforward way we can now reduce the single differences to their common fractional part by subtracting a rounded number of cycles and average the reduced single differences of all satellites. In order to avoid strong multipath influences and cycle slips at low elevations a large cut-off angle (e.g. 30°) has been used. This averaging gives the final estimate of the differential receiver clock error. A similar approach based on carrier phase single differences but introducing ambiguities, derived from a double-difference solution has been used in [7].

Because in practical applications the distances for remote clock comparisons are hundreds or thousands of kilometers it is in general necessary to use the ionosphere-free linear combination L3 of the two carrier frequencies L1 and L2

$$L_3 = \frac{f_1^2}{f_1^2 - f_2^2}\cdot L_1 - \frac{f_2^2}{f_1^2 - f_2^2}\cdot L_2\ . \quad (5)$$

Using this observable the first order effect of the ionospheric delay can be eliminated. Unfortunately, the observation noise of the L3 observations is usually three times larger compared to the original L1 observations.

B. Precise Point Positioning

Recently, time and frequency transfer using a geodetic analysis method known as Precise Point Positioning (PPP) has attracted much attention for clock comparisons [3]. The PPP solution is based on a combined analysis of dual-frequency code and carrier phase observations. Precise satellite orbits and clocks from the global IGS network are introduced and consistent models have to be applied. Station coordinates, tropospheric zenith delays, float ambiguities and the receiver clock offset with respect to the IGS timescale can then be estimated from the observation of a single station. Details on the modeling and parameter estimation can be found in [10]. The PPP approach has been proven to yield ITRF coordinates with an accuracy of 1-2 cm and receiver clock estimates with a precision of 100-200 ps. Because code and carrier phase observations are processed together, the consistency of these observation types is very important [5], [9].

IV. SINGLE DIFFERENCE RESULTS

A. Short term stability

In order to facilitate visual interpretation, data batches of only 4 hours recorded on the 20th and the 24th of December 2008 have been chosen for a detailed analysis of the tracking performance of the receivers. The data was collected in short and zero baseline mode, respectively. Prior to processing the observation data has been reduced to 30 s intervals. We selected satellite PRN 30 because it was observed both at low and high elevations during the observation window. The plots show L1 single differences.

On the short baseline we observe similar noise patterns in the single differences of the geodetic receivers (Fig. 3 and 4). The noise increases significantly at low elevations. This behavior is expected because at low elevations multipath effects are dominating over the receivers' measurement noise. In contrast, the noise of the single differences of the GTR50 receivers is much larger even at high elevations of the satellite (Fig. 5). This is probably due to the measurement noise of the internal time interval counter (TIC). According to the technical specifications of the receivers the TIC has a resolution of < 50 ps [11].

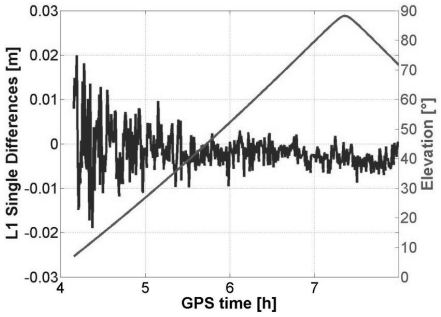

Figure 3. 4h of L1 single differences of PRN 30 as observed by the two JPS receivers on the short baseline

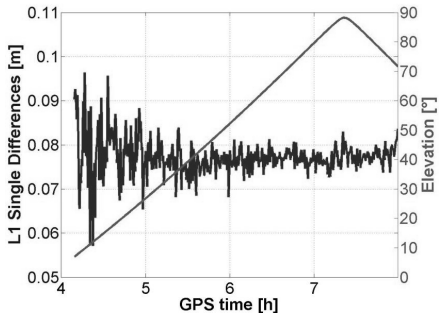

Figure 4. 4h of L1 single differences of PRN 30 as observed by the two Leica receivers on the short baseline

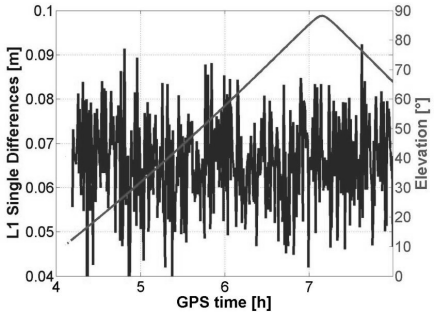

Figure 5. 4h of L1 single differences of PRN 30 as observed by the two DICOM receivers on the short baseline

On the zero baseline (Fig.6-8) we can observe a reduced noise level for the two geodetic receivers especially at low elevations. This demonstrates that station-specific effects, especially multipath influences, effectively cancel if both receivers share the same antenna. In addition, some very small long periodic deviations on top of the measurement noise become apparent. Again the single differences from the DICOM GTR50 receivers are dominated by the measurement noise.

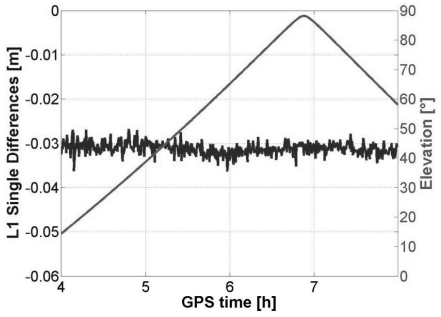

Figure 6. 4h of L1single differences of PRN 30 as observed by the two JPS receivers on the zero baseline

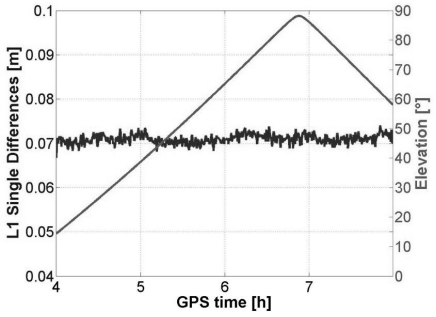

Figure 7. 4h of L1 single differences of PRN 30 as observed by the two Leica receivers on the zero baseline

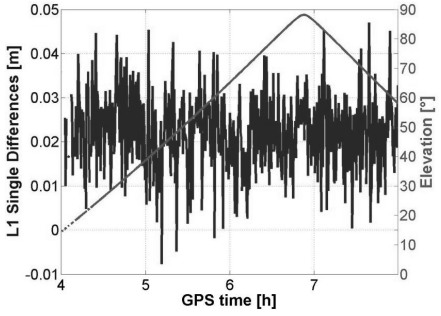

Figure 8. 4h of L1 single differences of PRN 30 as observed by the two DICOM receivers on the zero baseline

Tables II and III summarize the analysis of the 4h data batches in terms of RMS values. The single difference RMS values have been computed for the L1, L2 and L3 signals. The higher noise level of the DICOM receivers is evident. In the single differences of the geodetic receivers a higher noise level on the short baseline with respect to the zero baseline can be clearly seen. For example from the JPS data we infer an increase of the noise level by a factor of 2 on L1 and L2 and by a factor of 4 on the ionosphere-free linear combination L3. The typical amplification of the noise level on L3 by a factor of 3 with respect to L1 and L2 can only be found in the short baseline data. It has to be noted that the antennas in use are rather susceptible to multipath effects, due to their small ground planes.

TABLE II. SHORT BASELINE - SINGLE DIFFERENCE RMS

Receiver	L1 RMS [mm]	L2 RMS [mm]	L3 RMS [mm]
JPS Legacy	3.3	3.6	8.7
Leica GRX	3.1	3.3	8.4
DICOM GTR50	9.9	9.1	14.5

TABLE III. ZERO BASELINE – SINGLE DIFFERENCE RMS

Receiver	L1 RMS [mm]	L2 RMS [mm]	L3 RMS [mm]
JPS Legacy	1.4	1.8	2.2
Leica GRX	1.0	1.1	1.3
DICOM GTR50	9.0	8.8	10.0

B. Medium-term stability

In order to assess the stability of the differential receiver clock error over several days, a data set of 7 days from the zero baseline was processed in the way outlined in section III. For the JPS receiver we observe a 10 ps noise accompanied by a small non-linear drift (Fig. 9). This drift is not seen in the GTR50 data (Fig. 10) and cannot be explained, yet. The two spikes in the JPS data coincide with a loss of lock of the receivers, causing an integer cycle slip for all satellites.

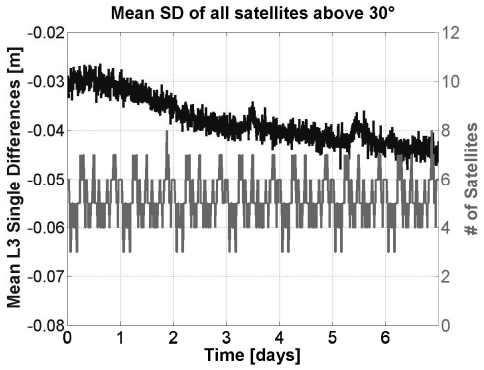

Figure 9. Mean L3 single differences of the JPS receivers on a zero baseline

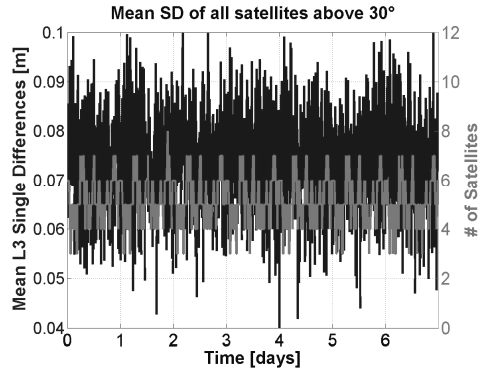

Figure 10. Mean L3 single differences of the DICOM receivers on a zero baseline

In order to characterize the noise of the differential clock errors of the three receivers, the Allan Deviation and the Modified Allan Deviation have been computed from the 7 days zero baseline data set. Inspecting the corresponding plots (Fig. 11 and 12) we can notice three characteristics:

- The GTR50 receiver is close to the behavior expected for an ideal receiver showing only white phase modulation (WPM) with a -3/2 slope in the log-log plot of the Modified Allan Dev. (Fig. 12) .
- For short averaging times however, the GTR50 receiver is almost one order of magnitude less precise than the geodetic receivers. For example six times more averaging time is required to reach the 10^{-15} level (Fig. 11).
- The JPS (Leica) receivers may provide an Allan Deviation of $\sigma_y(t) = 1 \cdot 10^{-16}$ ($2 \cdot 10^{-16}$) at one day averaging using L3 observations of a zero baseline, i.e. avoiding all environmental effects and thus indicating the internal system precision for this data set. Preliminary results from a 24 h short baseline L3 data set indicate an Allan Deviation of $4 \cdot 10^{-16}$ at one day averaging times for the JPS receivers.

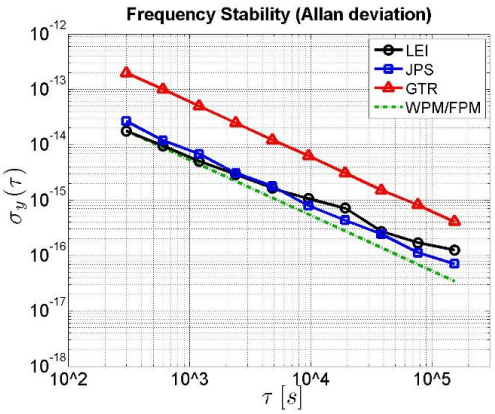

Figure 11. Allan Deviation of the differential clock error of the three receivers

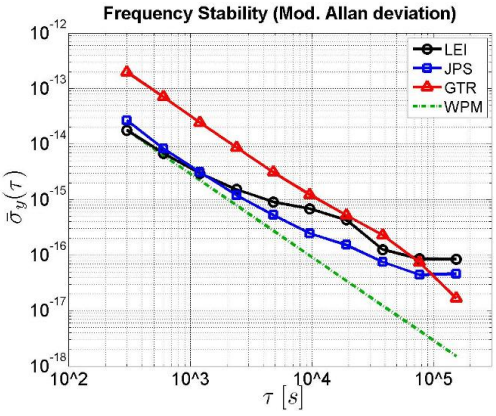

Figure 12. Modified Allan Deviation of the differential clock error of the three receivers

V. PRECISE POINT POSITIONING RESULTS

Figure 13 shows the differential clock offset of the two JPS receivers taken from a daily PPP solution. The well-known day-boundary jumps caused by the noise of the code signals can be observed. The size of these jumps is comparatively small (100 ps). This is, because the data was collected in a zero baseline setup, i.e. both receivers observed the same multipath errors. The remaining jumps are probably due to slightly different tracking of the individual receivers. At two epochs on the third and the sixth day a cycle slip for all satellites occurred, leading to an additional jump because the continuity of the phase ambiguities is interrupted. By manually removing all jumps and computing the Allan Deviation of the time series we could show a stability of $\sigma_y(\tau)=3\cdot10^{-16}$. This is slightly worse than the stability computed from the single differences. This could be caused by the estimation of tropospheric zenith path delays (ZPDs) in the PPP solution. The ZPD was estimated in 30 min intervals without additional constraints.

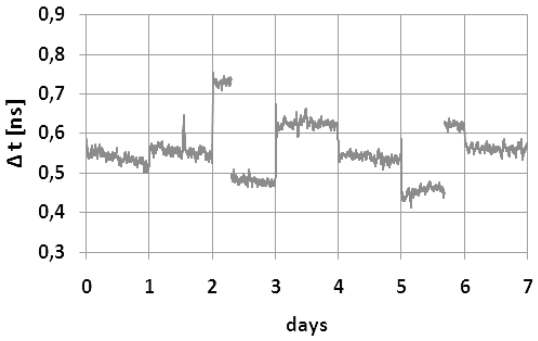

Figure 13. Differential clock offset of the JPS receivers computed in a daily PPP solution using the Bernese GPS software 5.0

VI. CONCLUSIONS

We tested three types of GPS receivers on their capability for frequency comparisons. We found significant differences between the geodetic receivers and the timing receivers. This is due to the fact that the timing receivers are fed only with a 1PPS signal, i.e. they are probably limited by the resolution of the internal time interval counter. In contrast the geodetic receivers show a much lower receiver clock noise level. This directly affects the performance of these receivers for frequency comparisons at short averaging times. On the other hand the medium-term and long-term stability of the GTR50 receivers is possibly superior to the clock stability of the geodetic receivers. However, longer data batches need to be analyzed to confirm this.

Using either of the two geodetic receivers connected to a common oscillator, a stability of the differential clock error of $\sigma_y(\tau)=2\cdot10^{-16}$ based on zero baseline L3 carrier phase observations has been demonstrated. Results from the short baseline test (Tab. II) indicate that multipath and other site dependent effects degrade the L3 observations of the JPS receivers by a factor of 4. Preliminary results based on a 24h data set suggest a stability of better than $\sigma_y(\tau)=4\cdot10^{-16}$ at one day averaging times on the short baseline. This is consistent with the corresponding RMS values (Tab. II) and the inferred stability floor of the geodetic technique stated in [12]. Thus we conclude that the capability of GNSS for frequency comparisons at the 10^{-16} level for one day averaging times is not limited by the receiver hardware, but rather environmental effects, such as multipath and tropospheric propagation delays. However, the drift observed in the differential receiver clock of some geodetic receivers needs further investigation.

DISCLAIMER

The authors do not attempt to recommend any of the instruments under test. It is also to be noted that the performance of the equipment presented in this paper depends on the particular environment and the individual receivers in use. Other receivers of the same type or the same manufacturer may show a different behavior. The reader is, however, encouraged to test his own equipment to identify the system performance with respect to a particular application.

ACKNOWLEDGMENT

We would like to thank Leica Geosystems for providing equipment and support.

REFERENCES

[1] J. Ray and K. Senior, "Geodetic techniques for time and frequency comparisons using GPS phase and code measurements," *Metrologia*, vol. 42, pp. 215-232, 2005

[2] K. Senior, P. Koppang, and J. Ray, "Developing an IGS time scale", *IEEE transactions on ultrasonics, ferroelectronics and frequency control*, 50(6), pp. 211-218, 2003

[3] G. Petit, E. F. Arias, "Use of IGS products in TAI applications," *Journal of Geodesy*, vol. 83, no. 3-4, pp. 327–334, 2009

[4] A. Bauch et al., "Comparison between frequency standards in Europe and the USA at the 10^{-15} uncertainty level," *Metrologia*, vol. 43, pp. 109–120, 2006

[5] R. Dach, T. Schildknecht, U. Hugentobler, L.G. Bernier, G. Dudle, "Continuous geodetic time-transfer analysis methods", *IEEE transactions on ultrasonics, ferroelectronics and frequency control* 53(7), pp. 1250-1259, July 2006

[6] E. Powers, P. Wheeler, D. Judge, and D. Matsakis, "Hardware Delay Measurements and Sensitivities in Carrier Phase Time Transfer," in *Proceedings of the 30th Annual Precise Time and Time Interval (PTTI) Systems and Appliations Meeting*, 1-3 December 1998, Reston, Virginia, USA, pp. 293-305, 1999

[7] C. Bruyninx, P. Defraigne, J.M. Sleewaegen "Time and Frequency transfer using GPS Code and Carrier Phases: Onsite Experiments", *GPS Solutions*, 3, pp. 1-10, 1999

[8] G. Petit, C. Thomas, Z. Jiang, P. Uhrich, F. Taris, "Use of GPS Ashtech Z12T receivers for accurate time and frequency comparisons", *IEEE Trans. UFFC*, Vol. 46-4, pp. 941-949, 1999

[9] D. Matsakis, M. Lee, R. Dach, U. Hugentobler, and Z. Jiang, "GPS carrier phase analysis noise on the USNO-PTB baselines," in *Proceedings of the IEEE International Frequency Control Symposium and Exposition*, pp. 631–636, Miami, Fla, USA, 2006

[10] J. Kouba and P. Héroux, "Precise Point Positioning Using IGS Orbit and Clock Products", *GPS Solutions*, vol. 5, pp. 12-28, 2001

[11] http://www.dicom.cz/en/product/873-time-frequency-transfer-receiver

[12] J. Ray and K. Senior, "IGS/BIPM pilot project: GPS carrier phase for time/frequency transfer and timescale formation", *Metrologia*, vol. 40, pp. 270-288, 2003